第 44 卷 第 5 期/2024 年 3 月/光学学报 研究论文

光学学报

基于TDLAS技术的人体呼出一氧化氮在线检测系统

何伟杰[1,2]，卢俊城[2]，高璐[2]，吴琼[2]，吴晓虞[3]，聂华贵[4]，陈孝敬[5**]，邵杰[2*]

[1]温州大学生命与环境科学学院，浙江 温州 325035；

[2]浙江师范大学浙江省光信息检测与显示技术研究重点实验室，浙江 金华 321004；

[3]浙江金华广福肿瘤医院，浙江 金华 321000；

[4]温州大学化学与材料工程学院，浙江 温州 325035；

[5]温州大学电子与电气工程学院，浙江 温州 325035

摘要 针对呼出气一氧化氮(FeNO)体积分数的检测，使用了具有高灵敏度、高精度等特性的可调谐半导体激光吸收光谱(TDLAS)技术。利用直接吸收光谱(DAS)技术和波长调制光谱(WMS)技术对呼出二氧化碳(CO_2)体积分数进行标定，并通过模拟两种气体信号来确定相关系数并完成FeNO体积分数反演。连续测量15 min气体体积分数，根据其变化实验和Allan方差曲线分析确定两种气体的参数，该系统中的CO_2气体测量精度和探测极限分别为0.045%和5.4×10^{-3}，一氧化氮(NO)气体测量精度和探测极限分别为1.1×10^{-9}和3.4×10^{-9}；通过反复置换CO_2和NO的混合气体与氮气(N_2)测量气体体积分数随时间变化情况来确定该系统响应时间为12 s；最后根据单次呼气周期曲线确定志愿者呼出气体中CO_2和NO的体积分数。该研究为FeNO的在线检测提供实验依据。

关键词 生物技术；光谱学；二氧化碳；一氧化氮；临床应用；吸收光谱

中图分类号 O657 **文献标志码** A **DOI**：10.3788/AOS231867

1 引 言

近年来，许多科学研究证明了人体呼出气一氧化氮(FeNO)体积分数可以作为一种生物标志物并应用于哮喘等呼吸道疾病的临床诊断中[1-2]。健康人群FeNO的体积分数一般低于2.5×10^{-8}，而哮喘等呼吸道疾病患者FeNO的体积分数高出健康人群2～10倍[3]。作为一种非侵入性、快捷和高效的呼气诊断方式，FeNO检测结果可以有效反应患者的气道炎症程度，以及预测患者的气道高反应性的急性加重和对皮质类固醇等生物疗法的反应[4-5]。由于人体FeNO的体积分数较小，且稳定性较差，极易氧化为二氧化氮(NO_2)，故对FeNO检测系统性能提出了严格要求。

调查研究表明，当前FeNO检测方法主要有化学发光法、电化学法和激光光谱法[6-9]等。化学发光法具有检测限低和灵敏度高的优点，被广泛应用于临床试验中，但其设备存在体积大且需要频繁校准等缺点[10-13]。虽然电化学技术设备具有更低的制造成本以及更轻便的设备，但电化学传感器属于消耗性材料，每个传感器在完成200次左右测量后就需要进行更换。这在一定程度上增加了使用成本，且该传感器也存在抗干扰性差的缺点[14-15]。

近年来，随着半导体激光器和光电探测器的飞速发展，可调谐半导体激光吸收光谱(TDLAS)技术因其具有高灵敏度、高精度等特性[16-19]，逐渐被应用于FeNO检测中[20]。2011年，Spagnolo等[21]基于石英增强光声光谱(QEPAS)技术以5.2 μm中红外量子级联激光器(QCL)为光源研制出一套时间分辨率为1 s、探测极限为8×10^{-9}的FeNO检测技术。由于呼出气体中的微小颗粒物易附着于传感器上，影响系统稳定性，因此，当使用QEPAS技术对FeNO进行检测时还需要另外的技术支持。2020年，北京协和医学院Ai等[22]将腔衰荡光谱(CRDS)技术运用在FeNO检测上，其探测极限为7.4×10^{-9}，并于次年证实了FeNO测量结果与肺癌疾病的相关性。但由于高反镜存在成本高和光路结构复杂等缺点，无法满足简单、便携式FeNO检测设备的需求。Namjou等[23]基于TDLAS技术搭建了一套FeNO检测系统，用Herriott池将系统的光程延

收稿日期：2023-12-01；**修回日期**：2023-12-26；**录用日期**：2024-01-05；**网络首发日期**：2024-02-20

基金项目：国家自然科学基金(61775797)、浙江省重点研发项目(2022C03066)、金华市重点科技攻关项目(20213032，2022-1-084，2022-3-071)

通信作者：*shaojie@zjnu.cn；**chenxj@wzu.edu.cn

长到 36 m，使系统的检测精度可达到 2.8×10^{-9}。相对于 CRDS 技术和 QEPAS 技术，TDLAS 技术具有更强的抗干扰能力和更简单的结构，所以更适合应用于 FeNO 检测设备。

本文以中心波长为 5263 nm 的 QCL 为光源、搭配光程为 26.8 m 的 Herriott 多通池[24]并结合 TDLAS 技术搭建了一套便携式 FeNO 检测系统，为 FeNO 实时在线检测提供数据支撑。

2 实验方法

2.1 基本原理

TDLAS 技术的基本理论是 Beer-Lamber 定律[25]。当光穿过一定体积分数的气体时，气体分子会吸收特定波长的光，出射光强度和入射光强度之间的关系表达式为

$$I(\nu)=I_0(\nu)\exp\left[-S(T)PXL\varphi(\nu)\right], \tag{1}$$

式中：ν 为激光频率，单位为 cm^{-1}；I 和 I_0 分别为出射光强度和入射光强度，单位为 mW；S 为温度等于 T 时的分子吸收线强，分子吸收线强的单位为 $cm^{-1}\cdot molecule^{-1}$，温度 T 的单位为 K；P 为压强，单位为 atm（1 atm=1.01×10^5 Pa）；X 为体积分数；L 为有效光程，单位为 cm；φ 为谱线线型函数。

直接吸收光谱（DAS）技术直接运用了 Beer-Lamber 定律。由于 DAS 技术易受到噪声干扰，常运用波长调制光谱（WMS）技术来提高系统的抗干扰能力。其实现方式为在激光进行扫描时叠加高频调制信号，经过调制后的信号由锁相放大器解调为二次谐波信号，其表达式[26]为

$$S_{2f}=-\beta I_D\alpha_0\frac{1}{4}m^2\chi, \tag{2}$$

式中：S_{2f} 为二次谐波信号的电信号强度，单位为 V；β 为信号放大系数；I_D 为光功率，单位为 mW；α_0 为光谱峰值吸收，单位为 cm^2；m 为调制系数；χ 为峰值归一化方程的二次谐波分量，当测量系统的压力和调制系数保持不变时，χ 可视为常数。

2.2 谱线选择

HITRAN（2023）数据库显示，能够满足体积分数较低的一氧化氮（NO）测量的吸收谱线位于 2.6 μm 和 5.2 μm 处。而 5.2 μm 附近的谱线线强比 2.6 μm 附近的高出一个数量级，且已被广泛应用于 NO 检测中[27-30]。考虑到人体呼出气体中含有 H_2O（体积分数约为 6%）和 CO_2（体积分数约为 4%），其波长谱线分布范围广，对 NO 吸收谱线产生影响。为了更好地进行 FeNO 测量，测量在 1899.8～1900.3 cm^{-1} 波数范围内的 NO（体积分数约为 5×10^{-9}）、CO_2 和 H_2O 的吸收光谱，如图 1 所示。其中光程为 26.88 m，温度为 296 K，压强为 0.3 atm。通过数据模拟可知，1900.07 cm^{-1} 处 NO 吸收谱线线强为 10^{-19} $cm^{-1}\cdot molecule^{-1}$，吸收谱线线强大于 10^{-21} $cm^{-1}\cdot molecule^{-1}$，可以满足体积分数低的 FeNO 测量要求；而 1899.95 cm^{-1} 处 CO_2 吸收谱线线强为 10^{-28} $cm^{-1}\cdot molecule^{-1}$，此处 NO 吸收谱线线强远高于 CO_2 吸收谱线线强。如图 1 中阴影部分所示，当压强为 0.3 atm 时，NO 吸收谱线和 CO_2 吸收谱线能够明显区分开，且 H_2O 无明显吸收。因此，选取该 1899.8～1900.3 cm^{-1} 范围内 CO_2 和 NO 吸收谱线作为目标谱线。

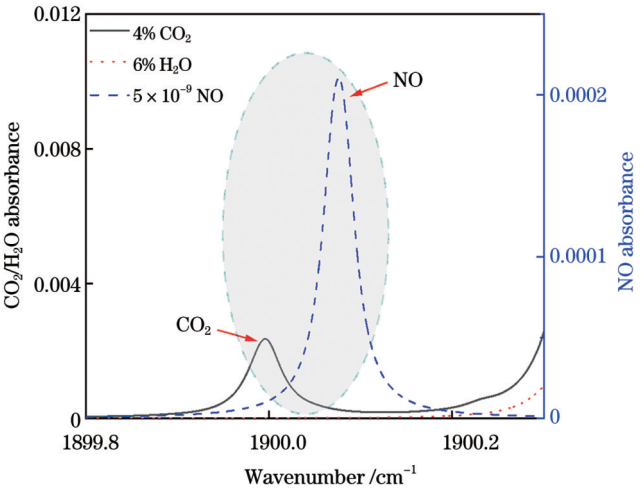

图 1 NO、CO_2 和 H_2O 吸收谱线分布

Fig. 1 Absorption spectral lines of NO, CO_2, and H_2O are distributed

2.3 系统组成

实验搭建的 FeNO 检测系统原理如图 2 所示。本系统所用光源为 QCL（宁波昕虹光电，QCL-C），通过激光驱动器（宁波昕虹光电，QC750-TouchTM）改变温度（20～50 ℃）和电流（450～750 mA）实现了波数从 1899.34 cm^{-1} 至 1906.57 cm^{-1} 的可调范围；通过函数发生器将高频（19520 Hz）正弦波和低频（9.3 Hz）三角波叠加形成输出信号并进入激光器完成波长扫描。激光经反射镜进入自制 Herriott 多通池反射 224 次，光程可达到 26.8 m。光电探测器（Vigo，PVI-2TE-6）接收出射光并将光信号转换为电信号，经由锁相放大器（Stanford research systems，SR830）解调放大后得到二次谐波信号（2f）。二次谐波信号由数据采集卡（北京星烁华创，FCFR-USB7020）采集并传输进入计算机（PC）完成处理分析。压力传感器（PS4-102V-Z）和流量传感器（炜盛电子科技，FR03H）分别实时监测气路中压强和流速，并利用真空泵和针阀进行控制和调整。

3 实验结果与分析

3.1 最优参数选择

在 WMS 技术中，调制振幅对气体吸收谱线的线宽有很大影响，因此需要确定最佳调制振幅。通入恒定体积分数为 4.76×10^{-6} 的 NO 气体，利用真空泵将多

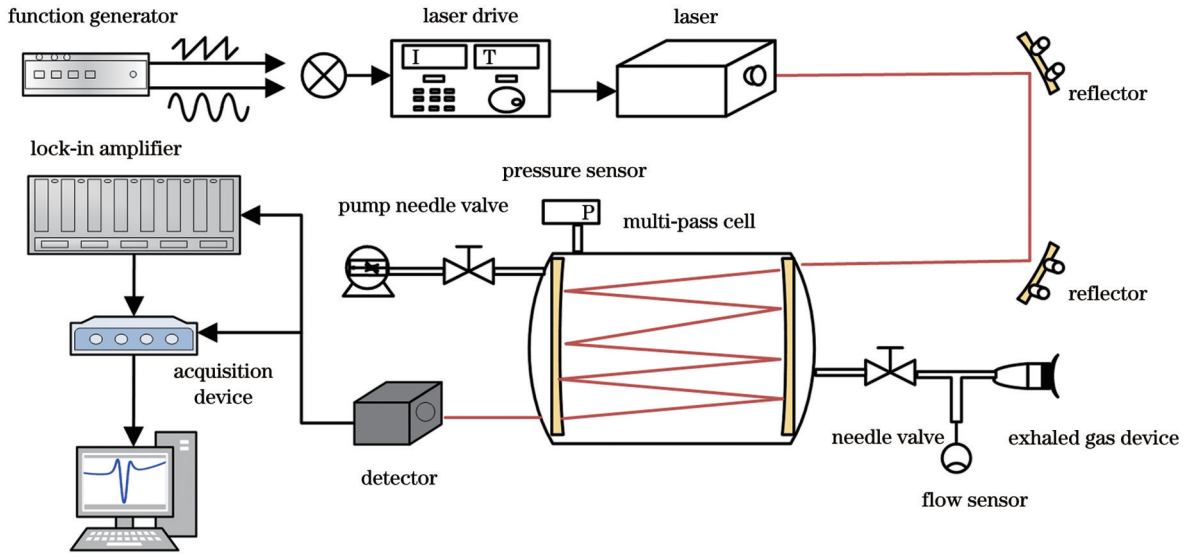

图 2　FeNO 检测系统原理图

Fig. 2　Schematic diagram of FeNO detection system

通池内压强控制在 0.3 atm 以内，改变调制振幅（10～50 mV），对应不同调制振幅的二次谐波信号峰值如图 3 所示。随着调制振幅的增加，二次谐波信号峰值增加速度趋于平缓，故该系统最佳调制振幅为 46 mV。

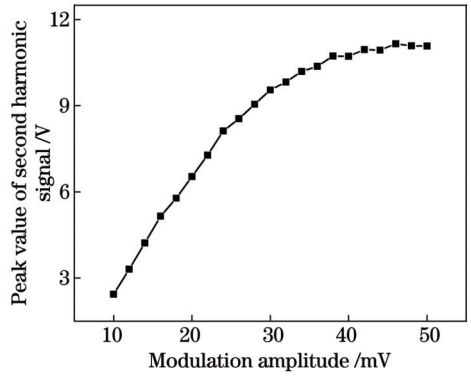

图 3　调制振幅与二次谐波信号峰值关系

Fig. 3　Relationship between modulation amplitude and peak value of second harmonic signal

3.2　系统标定

为了提高系统测量准确性，通过 DAS 技术和 WMS 技术对呼气过程中的两种气体进行标定。由式（1）可知，DAS 技术所得到的信号可直接推算出气体体积分数的大小。但由于人体 FeNO 的体积分数在 10^{-9} 量级，故无法使用该技术完成体积分数的反演。而 CO_2 在人体呼出气体中的体积分数约为 4%～6%，可以利用 DAS 技术完成气体标定。同时利用 DAS 技术和 WMS 技术测量人体呼出 CO_2 的信号峰值与体积分数，得到的结果如图 4 所示。

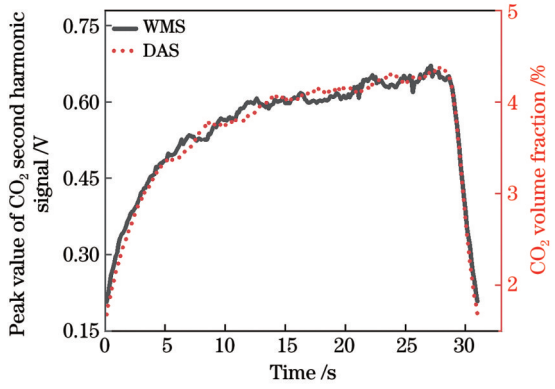

图 4　基于 WMS 技术和 DAS 技术的 CO_2 二次谐波信号峰值与体积分数曲线

Fig. 4　Peak value and volume fraction curves of CO_2 second harmonic signal based on WMS and DAS technologies

单次呼气周期内 CO_2 体积分数 X_{CO_2} 与二次谐波信号峰值 S_{CO_2} 关系如图 5 所示，其表达式为

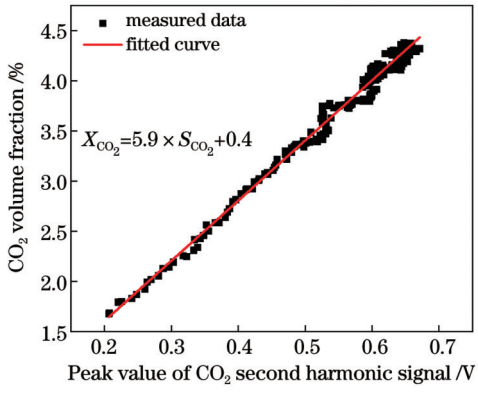

图 5　CO_2 体积分数与二次谐波信号峰值关系

Fig. 5　Relationship between CO_2 volume fraction and peak value of second harmonic signal

$$X_{CO_2}=5.9\times S_{CO_2}+0.4。\tag{3}$$

当系统调制振幅与压强恒定时，存在系数 A 使

CO_2和NO二次谐波信号与体积分数满足关系

$$A_{NO}\cdot S_{NO}=X_{NO},\tag{4}$$

$$A_{CO_2}\cdot S_{CO_2}=X_{CO_2},\tag{5}$$

$$A\cdot\frac{S_{NO}}{S_{CO_2}}=\frac{X_{NO}}{X_{CO_2}}。\tag{6}$$

在单次呼气周期内，当系统条件不发生改变时，系数A也始终不变。模拟人体呼出CO_2（体积分数为4%）和NO（体积分数为2.0×10^{-8}）的二次谐波信号强度，结果如图6所示，根据式(6)计算出系数A为

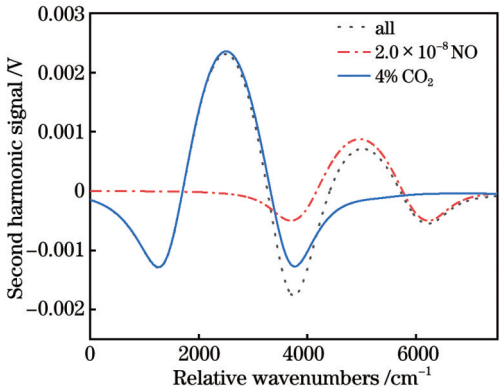

图6　体积分数为4%的CO_2和体积分数为2.0×10^{-8}的NO的二次谐波信号模拟

Fig. 6　Simulation of second harmonic signals for CO_2 with a volume fraction of 4% and NO with a volume fraction of 2.0×10^{-8}

1318.8，则NO体积分数的表达式为

$$X_{NO}=1318.8\cdot\frac{S_{NO}}{S_{CO_2}}\cdot X_{CO_2}。\tag{7}$$

基于式(7)，计算得出单次呼气周期内NO体积分数X_{NO}与二次谐波信号峰值S_{NO}关系如图7所示。

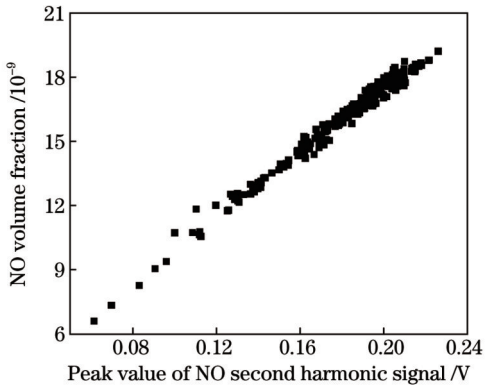

图7　NO体积分数与二次谐波信号峰值关系

Fig. 7　Relationship between NO volume fraction and peak value of second harmonic signal

3.3　系统性能分析

3.3.1　测量精度

为了更好地分析系统测量值与真实值的误差，进行测量精度实验。向多通池内通入CO_2和NO混合气体，并对气体进行连续15 min的测量，两种气体的测量结果如图8所示。系统测量CO_2体积分数平均值为3.1%，精度为0.045%，相对误差（测量精度/气体体积分数平均值）为1.4%。系统测量NO体积分数平均值为14.8×10^{-9}，精度为1.1×10^{-9}，相对误差（测量精度/气体体积分数平均值）为7.4%。由测量结果的数据分析可知，系统测量精度满足FeNO在线检测的要求。

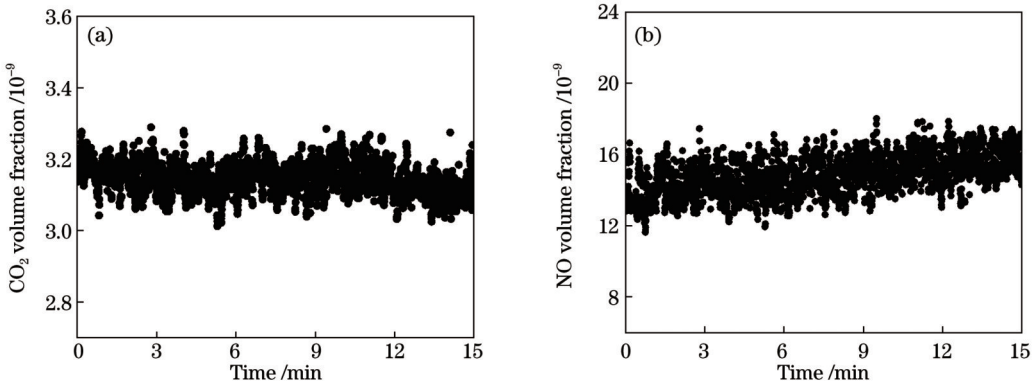

图8　15 min连续测量气体体积分数变化。(a) CO_2；(b) NO

Fig. 8　Continuous measurement of gas volume fraction variations for 15 min. (a) CO_2; (b) NO

3.3.2　响应时间

所采用的呼气检测方式为实时在线检测，为了保证实验测量数据的完整性和准确性，故需要对系统响应时间进行测量。通过切换质量流量计的气体控制阀门交替通入CO_2和NO的混合气体与N_2，通气时间均为90 s，连续进行3次实验。得到的系统响应曲线如图9所示。二次谐波信号峰值上升和下降的响应时间均为12 s（图9中的阴影区域），而成年人一次完整的呼气周期在20 s以上，所以能够证明此系统可以实现实时在线检测。

3.3.3　系统稳定性

为了探究系统稳定性并分析探测极限，实验对体积分数为5%的CO_2以及体积分数为2.0×10^{-8}的NO进行1 h测量，并且对测量结果进行Allan方差分析，

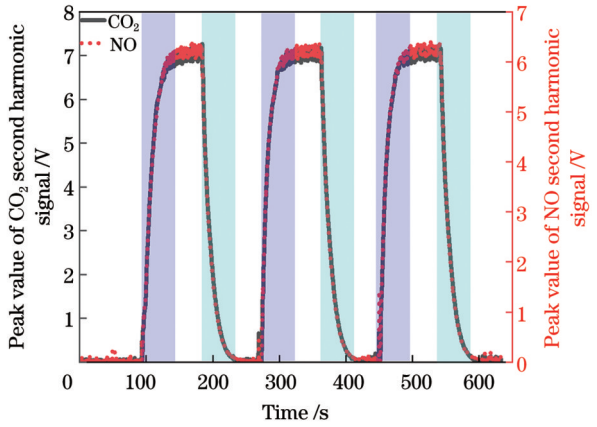

图 9　系统响应曲线

Fig. 9　System response curve

实验结果如图 10 所示。由 Allan 曲线可知，该系统的最佳积分时间为 25 s，系统 CO_2 检测极限为 5.4×10^{-3}，系统 NO 检测极限为 3.4×10^{-9}。由美国胸腔学会（ATS）所提出的标准可知，患有呼吸道疾病的患者和健康人群呼出 NO 体积分数区分界限在 2.5×10^{-8}。实验结果表明，NO 检测极限小于 2.5×10^{-8}，本系统满足人体呼出 NO 检测的研究要求。

3.4　应用示范

美国胸腔学会和中国哮喘联盟建议在 FeNO 在线检测实验前 1 h 被检测者应禁食，且检测时呼气流速应保持在 3 L/min。如图 11 所示，成年人单次完整呼气周期中 CO_2 和 NO 体积分数变化曲线，可分为上升期、平台期和下降期三阶段。参照美国胸腔学会和欧洲呼吸学会（ERS）建议，该系统选取第二阶段的体积分数平均值作为测量结果。

选取 18 名志愿者按照上述检测要求进行在线 FeNO 检测实验，得到 CO_2 和 NO 体积分数如图 12 所示，FeNO 测量体积分数均低于 25×10^{-9}，其结果满足美国胸腔学会提出的标准。

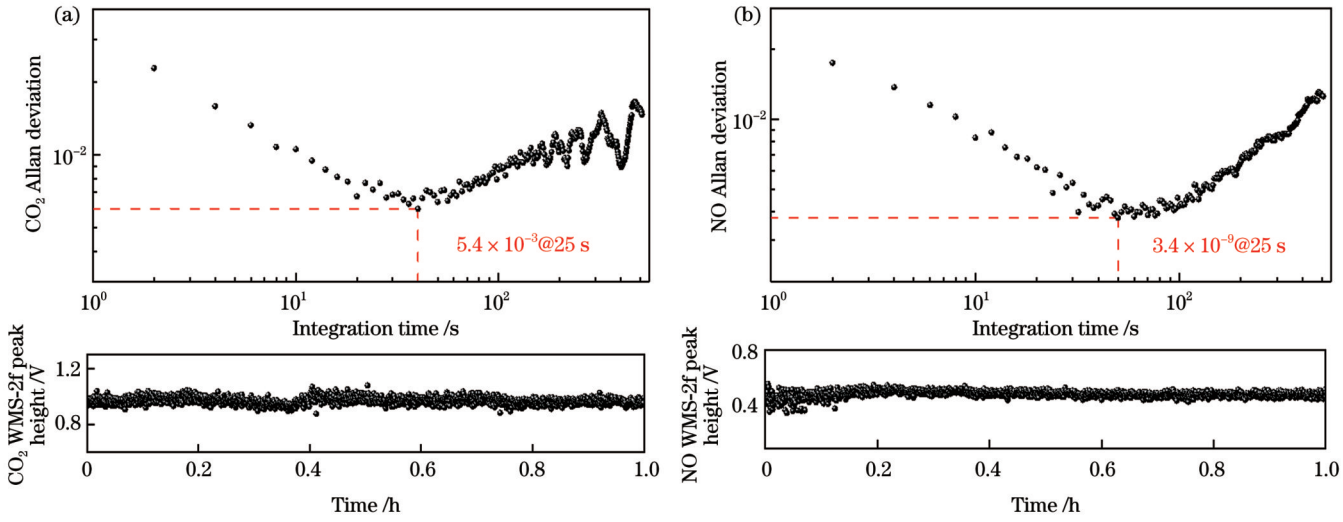

图 10　气体体积分数连续测量结果和 Allan 方差。(a) CO_2；(b) NO

Fig. 10　Continuous measurement results of gas volume fraction and Allan variance. (a) CO_2; (b) NO

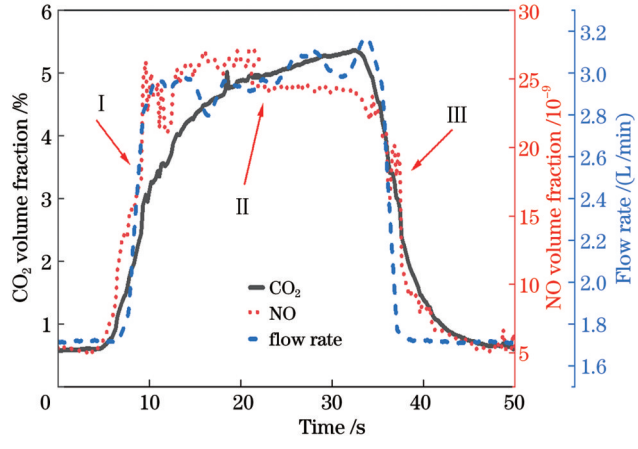

图 11　单次呼气周期 CO_2 和 NO 体积分数变化曲线

Fig. 11　Curves CO_2 and NO volume fractions during single exhalation cycle

4　结　　论

基于 TDLAS 技术搭建了一套 FeNO 检测系统，所选取的 NO 目标吸收谱线在 1900.07 cm^{-1} 波数处。在压强为 0.3 atm 的条件下，对体积分数为 4.76×10^{-6} 的 NO 进行试验并选取 46 mV 作为实验最优调制振幅。利用 DAS 技术和 WMS 技术对 CO_2 体积分数进行标定，并通过模拟二次谐波信号计算 CO_2 与 NO 信号之间的关系，完成对 NO 体积分数的标定。为了评估该系统的性能，分别对气体 CO_2 和 NO 的测量精度、响应时间和稳定性进行分析。通过 Allan 方差分析，当积分时间为 25 s 时，系统对 CO_2 和 NO 的检测极限分别为 5.4×10^{-3} 和 3.4×10^{-9}。最后根据成年人完整呼气周期分析不同阶段 CO_2 和 NO 的体积分数，并对 18 个志愿者样本进行处理分析。实验结果证明利

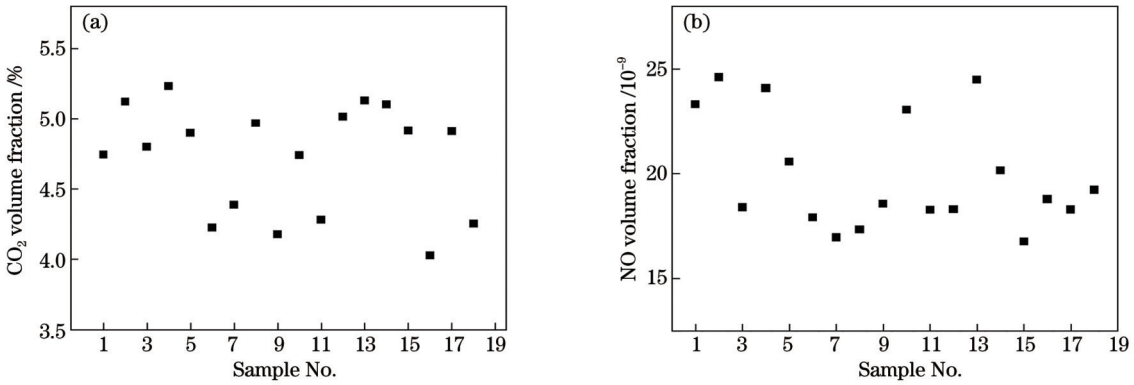

图 12 志愿者呼出气体体积分数测量结果。(a) CO_2;(b) NO

Fig. 12 Measurement results of volume fraction of exhaled gas by volunteers. (a) CO_2; (b) NO

用中红外 QCL 对体积分数较低的 NO 进行测量具有可行性,为人体呼出气体实时在线检测提供参考依据。

参 考 文 献

[1] 孙晓丽, 张湘华, 曹晓玮. 呼出气一氧化氮对支气管哮喘的诊断价值及其与疾病严重程度的关系[J]. 中国医药导报, 2020, 17(22): 82-85.
Sun X L, Zhang X H, Cao X W. The diagnostic value of fractional exhaled nitric oxide in bronchial asthma and its relationship with disease severity[J]. China Medical Herald, 2020, 17(22): 82-85.

[2] Chen L C, Wu L L, Lu D Z, et al. The value of fractional exhaled nitric oxide and impulse oscillometric and spirometric parameters for predicting bronchial hyperresponsiveness in adults with chronic cough[J]. Journal of Asthma and Allergy, 2021, 14: 1065-1073.

[3] 中国医药教育协会慢性气道疾病专业委员会, 中国哮喘联盟. 呼出气一氧化氮检测及其在气道疾病诊治中应用的中国专家共识[J]. 中华医学杂志, 2021, 101(38): 3092-3114.
Chronic Airway Disease Specialized Committee of China Medical Education Association, China Asthma Alliance. China expert consensus on exhaled breath nitric oxide detection and its application in the diagnosis and management of airway diseases [J]. National Medical Journal of China, 2021, 101(38): 3092-3114.

[4] Tiotiu A. Biomarkers in asthma: state of the art[J]. Asthma Research and Practice, 2018, 4: 10.

[5] Paro-Heitor M L Z, Bussamra M H C F, Saraiva-Romanholo B M, et al. Exhaled nitric oxide for monitoring childhood asthma inflammation compared to sputum analysis, serum interleukins and pulmonary function[J]. Pediatric Pulmonology, 2008, 43(2): 134-141.

[6] Maniscalco M, Vitale C, Vatrella A, et al. Fractional exhaled nitric oxide-measuring devices: technology update[J]. Medical Devices, 2016, 9: 151-160.

[7] Cristescu S M, Mandon J, Harren F J M, et al. Methods of NO detection in exhaled breath[J]. Journal of Breath Research, 2013, 7(1): 017104.

[8] Wang C J, Sahay P. Breath analysis using laser spectroscopic techniques: breath biomarkers, spectral fingerprints, and detection limits[J]. Sensors, 2009, 9(10): 8230-8262.

[9] Borrill Z, Clough D, Truman N, et al. A comparison of exhaled nitric oxide measurements performed using three different analysers[J]. Respiratory Medicine, 2006, 100(8): 1392-1396.

[10] Mandon J, Högman M, Merkus P J F M, et al. Exhaled nitric oxide monitoring by quantum cascade laser: comparison with chemiluminescent and electrochemical sensors[J]. Journal of Biomedical Optics, 2012, 17(1): 017003.

[11] Dunlea E J, Herndon S C, Nelson D D, et al. Evaluation of nitrogen dioxide chemiluminescence monitors in a polluted urban environment[J]. Atmospheric Chemistry and Physics, 2007, 7(10): 2691-2704.

[12] Wany A, Gupta A K, Kumari A, et al. Chemiluminescence detection of nitric oxide from roots, leaves, and root mitochondria[J]. Methods in Molecular Biology, 2016, 1424: 15-29.

[13] Menou A, Babeanu D, Paruit H N, et al. Normal values of offline exhaled and nasal nitric oxide in healthy children and teens using chemiluminescence[J]. Journal of Breath Research, 2017, 11(3): 036008.

[14] Brooks C R, Brogan S B M, van Dalen C J, et al. Measurement of exhaled nitric oxide in a general population sample: a comparison of the Medisoft HypAir FE_{NO} and Aerocrine NIOX analyzers[J]. The Journal of Asthma, 2011, 48(4): 324-328.

[15] Mandon J, Högman M, Merkus P J F M, et al. Quantum cascade laser for breath analysis: application to nitric oxide monitoring[C]//Lasers, Sources, and Related Photonic Devices, January 29-February 1, 2012, San Diego, California. Washington, DC: OSA, 2012: LM3B.6.

[16] 徐俊, 李云飞, 程跃, 等. 基于 TDLAS-WMS 的甲烷泄漏遥测系统研制[J]. 激光与光电子学进展, 2023, 60(6): 0628006.
Xu J, Li Y F, Cheng Y, et al. Development of methane leakage telemetry system based on TDLAS-WMS[J]. Laser & Optoelectronics Progress, 2023, 60(6): 0628006.

[17] 辛文辉, 任卓勇, 樊建鑫, 等. 基于 FPGA 的 TDLAS-WMS 信号控制系统设计及实现[J]. 激光与光电子学进展, 2023, 60(5): 0530001.
Xin W H, Ren Z Y, Fan J X, et al. Design and implementation of a field programmable gate array-based signal control system for tunable diode laser absorption spectroscopy-wavelength modulation spectroscopy[J]. Laser & Optoelectronics Progress, 2023, 60(5): 0530001.

[18] 王鑫, 荆聪蕊, 侯凯旋, 等. 基于 TDLAS 技术的人体呼气末 CO_2 在线检测[J]. 中国激光, 2020, 47(3): 0311002.
Wang X, Jing C R, Hou K X, et al. Online detection of human-exhaled end-tidal carbon dioxide using tunable semiconductor absorption spectroscopy[J]. Chinese Journal of Lasers, 2020, 47(3): 0311002.

[19] 王宣, 高光珍, 龙芳宇, 等. 基于波长调制腔增强吸收光谱技术的 CO 体积分数测量[J]. 中国激光, 2023, 50(13): 1311001.
Wang X, Gao G Z, Long F Y, et al. CO volume fraction measurement based on wavelength modulated cavity-enhanced absorption spectroscopy[J]. Chinese Journal of Lasers, 2023, 50(13): 1311001.

[20] 李玫仪, 王飞, 张雅琪. 基于中红外激光吸收光谱的低浓度一氧化氮测量[J]. 激光与光电子学进展, 2018, 55(5): 053002.
Li M Y, Wang F, Zhang Y Q. Measurement of nitric oxide with low concentration based on mid-infrared laser absorption spectroscopy[J]. Laser & Optoelectronics Progress, 2018, 55(5): 053002.
[21] Spagnolo V, Lewicki R, Dong L, et al. Quantum-cascade-laser-based optoacoustic detection for breath sensor applications[C]// 2011 IEEE International Symposium on Medical Measurements and Applications, May 30-31, 2011, Bari, Italy. New York: IEEE Press, 2011: 332-335.
[22] Ai Y K, Li J, Li Q Y, et al. Cavity ringdown spectroscopy of nitric oxide in the ultraviolet region for human breath test[J]. Journal of Breath Research, 2020, 14(3): 037101.
[23] Namjou K, Roller C B, Reich T E, et al. Determination of exhaled nitric oxide distributions in a diverse sample population using tunable diode laser absorption spectroscopy[J]. Applied Physics B, 2006, 85(2): 427-435.
[24] Liu Y H, Ma Y F. Advances in multipass cell for absorption spectroscopy-based trace gas sensing technology[J]. Chinese Optics Letters, 2023, 21(3): 033001.
[25] Xin Z. Diode laser absorption sensors for combustion control[D]. Stanford: Stanford University, 2005.
[26] Kluczynski P, Gustafsson J, Lindberg Å M, et al. Wavelength modulation absorption spectrometry: an extensive scrutiny of the generation of signals[J]. Spectrochimica Acta Part B: Atomic Spectroscopy, 2001, 56(8): 1277-1354.
[27] Zhou S, Han Y L, Li B C. Pressure optimization of an EC-QCL based cavity ring-down spectroscopy instrument for exhaled NO detection[J]. Applied Physics B, 2018, 124(2): 27.
[28] Rieker G B, Jeffries J B, Hanson R K. Calibration-free wavelength-modulation spectroscopy for measurements of gas temperature and concentration in harsh environments[J]. Applied Optics, 2009, 48(29): 5546-5560.
[29] McCurdy M R, Bakhirkin Y A, Wysocki G, et al. Performance of an exhaled nitric oxide and carbon dioxide sensor using quantum cascade laser-based integrated cavity output spectroscopy[J]. Journal of Biomedical Optics, 2007, 12(3): 034034.
[30] Petralia L S, Bahl A, Peverall R, et al. Accurate real-time $F_{E}NO$ expirograms using complementary optical sensors[J]. Journal of Breath Research, 2020, 14(4): 047102.

Online Detection System of Human Exhaled Nitric Oxide Based on TDLAS Technology

He Weijie[1,2], Lu Juncheng[2], Gao Lu[2], Wu Qiong[2], Wu Xiaoyu[3], Nie Huagui[4], Chen Xiaojing[5**], Shao Jie[2*]

[1]*College of Life and Environmental Science, Wenzhou University, Wenzhou* 325035, *Zhejiang, China*;
[2]*Key Laboratory of Researching Optical Information Detecting and Display Technology in Zhejiang Province, Zhejiang Normal University, Jinhua* 321004, *Zhejiang, China*;
[3]*Zhejiang Jinhua Guangfu Tumor Hospital, Jinhua* 321000, *Zhejiang, China*;
[4]*College of Chemistry & Materials Engineering, Wenzhou University, Wenzhou* 325035, *Zhejiang, China*;
[5]*College of Electrical and Electronic Engineering, Wenzhou University, Wenzhou* 325035, *Zhejiang, China*

Abstract

Objective In recent years, death and economic losses caused by respiratory diseases have occurred globally, with a significant portion of respiratory disease patients facing challenges related to delayed early detection and inadequate treatment in later stages. With the advancing medical technology, numerous studies have demonstrated a close association between the volume fraction of human fractional exhaled nitric oxide (FeNO) and respiratory disease. In normal individuals, airway epithelial cells produce a small amount of nitric oxide (NO), with volume fractions generally below 2.5×10^{-8}. However, in patients with respiratory diseases, inflammatory cells in the airways produce a large amount of NO, with volume fractions generally 2–10 times higher than those in normal individuals. FeNO detection is a non-invasive, simple, rapid, and efficient method for exhaled breath diagnosis. It can be employed to differentiate respiratory diseases with similar clinical presentations, such as asthma, chronic obstructive pulmonary disease (COPD), and overlapping syndromes. Additionally, it can predict treatment outcomes and post-treatment management for patients with these conditions. FeNO detection provides information that cannot be obtained from medical history, physical examinations, and lung function tests alone, and it contributes to improving the diagnosis and treatment of respiratory diseases, elevating the clinical management of respiratory diseases to a new height.

Methods For FeNO detection, we utilize tunable diode laser absorption spectroscopy (TDLAS) technology, which is known for its high sensitivity, precision, and fast response rate. The fundamental theory of TDLAS is based on Beer-Lambert's law that when light passes through a certain volume fraction of gas, gas molecules absorb light at specific wavelengths. The relationship between the emitted light intensity and incident light intensity can be directly adopted to

establish the relationship between the signal magnitude and gas molecule volume fraction. Direct absorption spectroscopy (DAS) directly applies this law. Due to the susceptibility of DAS to low-frequency noise such as interference fringes, wavelength modulation spectroscopy (WMS) is a commonly adopted method to suppress low-frequency noise. The basic principle of a WMS involves the combination of a low-frequency triangular wave signal and a high-frequency sine wave signal generated by a signal generator. These signals are introduced into the laser to drive both scanning and modulation of the laser wavelength, and the laser is directed into the gas absorption cell, interacting with gas molecules. The detector receives the laser light after the interaction and converts the optical signal into an electrical signal, and the lock-in amplifier demodulates it into a harmonic signal. The relationship between the harmonic signal and gas molecule volume fraction is established by gas calibration.

Results and Discussions We calibrate the exhaled carbon dioxide (CO_2) volume fraction within a single exhalation cycle using both DAS and WMS (Figs. 4 and 5). By simulating the second harmonic signals of mixed gases of CO_2 and NO, we determine correlation coefficients to achieve the inversion of FeNO volume fraction (Figs. 6 and 7). By a 15-minute continuous measurement of the volume fraction changes of mixed gases of CO_2 and NO, and Allan variance curve analysis, the system's CO_2 gas measurement precision and detection limit are determined to be 0.045% and 5.4×10^{-3} [Figs. 8(a) and 10(a)] respectively. For NO, the measurement precision and detection limit are found to be 1.1×10^{-9} and 3.4×10^{-9} [Figs. 8(b) and 10(b)], respectively. By repeatedly replacing mixed gases of CO_2 and NO with nitrogen (N_2) and measuring the gas volume fraction changes over time, the system's response time is determined to be 12 s (Fig. 9). Finally, based on the gas curve during a single exhalation cycle at an exhalation flow rate of 3 L/min, the volume fractions of CO_2 and NO in the exhaled breath of 18 volunteers are determined (Figs. 11 and 12).

Conclusions We establish a FeNO detection system based on TDLAS, with the selected target absorption line for NO at a wavenumber of 1900.07 cm^{-1}. Experimentation is conducted with NO at a volume fraction of 4.76×10^{-6} under a pressure of 0.3 atm, and 46 mV is chosen as the optimal modulation amplitude. DAS and WMS are adopted to calibrate the CO_2 volume fraction. By simulating the second harmonic signals, we calculate the relationship between the signals of CO_2 and NO, completing NO volume fraction calibration. Precision, response time, and stability of both CO_2 and NO are analyzed to evaluate the system performance. Through Allan variance analysis, within an integration time of 25 s, the system's detection limits for CO_2 and NO are determined to be 5.4×10^{-3} and 3.4×10^{-9} respectively. Finally, an analysis of different stages of the complete exhalation cycle in adults is conducted to calculate the concentrations of CO_2 and NO, and 18 volunteer samples are processed and analyzed. Experimental results demonstrate the feasibility of using a mid-infrared quantum cascade laser (QCL) for low-concentration measurement of NO, providing references for real-time online detection of human exhaled gases.

Key words biotechnology; spectroscopy; carbon dioxide; nitric oxide; clinical applications; absorption spectroscopy